CONCLUSION

Lymphoscintigraphy by injecting a small volume (0.4 ml) of radiolabeled colloid (size range 200–1000 nm) can be used in association with GDP-guided SN biopsy to provide reliable information on the state of the axillar for staging purposes. Both the subdermal and peritumoral colloid administration routes are acceptable, although the subdermal route appears superior. The technique is simple to perform, relatively inexpensive and well accepted by patients. We hope that may be used as part of a less-aggressive approach to breast cancer that does not compromise the curative intent of the treatment.

ACKNOWLEDGMENTS

We thank Laura Cordini for typing this article and Don Ward for help with the English. This work was supported by grants from the Italian Association for Cancer Research.

REFERENCES

1. Veronesi U, Salvadori B, Luini A, et al. Conservative treatment of early breast cancer. Long term results of 1232 cases treated with quadrantectomy, axillary dissection and radiotherapy. *Ann Surg* 1990;211:250–259.
2. Greco M, Agresti R, Raselli L, Giovanazzi R, Veronesi U. Axillary dissection can be avoided in selected breast cancer patients. Analysis of 401 cases. *Anticancer Res* 1996;16:3913–3918.
3. Silverstein MJ, Gierson ED, Waisman JR, Senoksky GM, Colburm WJ, Gamagami P. Axillary lymph node dissection for T1a breast carcinoma. Is it indicated? *Cancer* 1994;73:664–667.
4. Tubiana M, Holland R, Kopans DB, et al. Commission of the European Communities "Europe Against Cancer" Programme. European School of Oncology Advisory Report. Management of non-palpable and small lesions found in mass breast screening. *Eur J Cancer* 1994;30:538–547.
5. Morton D, Wen D, Cochran A. Management of early-stage melanoma by intraoperative lymphatic mapping and selective lymphadenectomy: an alternative to routine elective lymphadenectomy or "watch and wait." *Surg Oncol Clin North Am* 1992;1: 247–259.
6. Morton D, Wen D, Wong J, et al. Technical details of intraoperative lymphatic mapping for early stage melanoma. *Arch Surg* 1992;127:392–399.
7. Giuliano AE, Kirgan DM, Guenther JM, Morton DL. Lymphatic mapping and sentinel lymphadenectomy for breast cancer. *Ann Surg* 1994;220:391–401.
8. Pettaway CA, Pisters LL, Dinney CP, et al. Sentinel lymph node dissection for penile carcinoma: the M.D. Anderson Cancer Center experience. *J Urol* 1995;154:1999–2003.
9. Levenback C, Burke TW, Morris M, Malpica A, Lucas KR, Gershenson DM. Potential applications of intraoperative lymphatic mapping in vulvar cancer. *Gynecol Oncol* 1995;59:216–220.
10. Giuliano AE, Dale PS, Turner RR, Morton DL, Evans SW, Krasne DL. Improved axillary staging of breast cancer with sentinel lymphadenectomy. *Ann Surg* 1995;222: 394–401.
11. Giuliano AE. Sentinel lymphadenectomy in primary breast carcinoma: an alternative to routine axillary dissection. *J Surg Oncol* 1996;62:75–77.
12. Van der Veen H, Hoekstra OS, Paul MA, Cuesta MA, Meijer S. Gamma probe-guided sentinel node biopsy to select patients with melanoma for lymphadenectomy. *Br J Surg* 1994;81:1769–1770.
13. Krag DN, Weaver DL, Alex JC, Fairbank JT. Surgical resection and radiolocalization of the sentinel lymph node in breast cancer using a gamma probe. *Surg Oncol* 1993;2:335–340.
14. Albertini JJ, Lyman GH, Cox C, et al. Lymphatic mapping and sentinel node biopsy in the patient with breast cancer. *JAMA* 1996;276:1818–1822.
15. Pijpers R, Meijer S, Hoekstra OS, et al. Impact of lymphoscintigraphy on sentinel node identification with technetium-99m-colloidal albumin in breast cancer. *J Nucl Med* 1997;38:366–368.
16. De Cicco C, Cremonesi M, Chinol M, et al. Optimization of axillary lymphoscintigraphy to detect the sentinel node in breast cancer. *Tumori* 1997;83:539–541.
17. ICRP. *International Commission on Radiological Protection Publ. No. 60.* Oxford: Pergamon Press; 1991.
18. Alazraki NP, Eshima D, Eshima LA, et al. Lymphoscintigraphy, the sentinel node concept, and the intraoperative gamma probe in melanoma, breast cancer and other potential cancers. *Semin Nucl Med* 1997;37:55–67.
19. Eshima D, Eshima LA, Herda SC, et al. Preparation and evaluation of ^{99m}Tc sulfur colloid for lymphoscintigraphy studies [Abstract]. *J Nucl Med* 1996;37:84P.
20. Smith F, Ramos-Gabatin A, Olalde L. Reduced particle size sulfur colloid for lymphoscintigraphy [Abstract]. *J Nucl Med* 1996;37:301P.
21. Uren RF, Howman-Giles RB, Thompson JF, et al. Mammary lymphoscintigraphy in breast cancer. *J Nucl Med* 1995;36:1775–1780.
22. El-Shirbiny AM, S Yeh HS Cody, Borgen PI, Larson SM. Scintigraphic identification of sentinel lymph node in breast carcinoma [Abstract]. *Eur J Nucl Med* 1997;24:892.
23. Veronesi U, Paganelli G, Galimberti V, et al. Sentinel-node biopsy to avoid axillary dissection in breast cancer with clinically negative lymph-nodes. *Lancet* 1997;349: 1864–1867.

Fluorine-18-Fluorodeoxyglucose PET Identification of Cardiac Metastasis Arising from Uterine Cervical Carcinoma

Yoriko Shimotsu, Yoshio Ishida, Kazuki Fukuchi, Kohei Hayashida, Masahiro Toba, Seiki Hamada, Makoto Takamiya, Toru Satoh, Norifumi Nakanishi and Tsunehiko Nishimura

Departments of Radiology and Cardiology, National Cardiovascular Center; and Division of Tracer Kinetics, Biomedical Research Center, Osaka University Medical School, Osaka, Japan

Cardiac metastasis of uterine cervical carcinoma is rare. We describe a patient with a past history of uterine cervical carcinoma who presented with metastasis to the heart, lungs and distant lymph nodes 3 yr after surgery and chemotherapy. Since the patient complained of chest pain and demonstrated electrocardiogram abnormalities, we performed echocardiography, electron beam CT and MRI, which revealed a tumor in the right ventricular wall. The tumor was assessed by ^{67}Ga scintigraphy and ^{18}F-fluorodeoxyglucose (FDG) PET scanning. The mean differential ^{18}F-FDG uptake ratio of the tumor was 7.9, suggesting malignancy, which was later confirmed by myocardial biopsy. Information about the extent of the tumor and partial necrosis within it was provided by ^{18}F-FDG PET. Although both radionuclide imaging techniques also detected metastatic lesions in the lungs and lymph nodes, ^{18}F-FDG PET scanning detected small lesions more sensitively than ^{67}Ga scintigraphy.

Key Words: heart neoplasm; uterine carcinoma; fluorine-18-fluorodeoxyglucose

J Nucl Med 1998; 39:2084–2087

Uterine cervical carcinoma often spreads to the vaginal mucosa and the myometrium of the lower uterine segment (*1*). Sometimes it metastasizes to distant organs such as the lung, bone and brain (*2*), but metastasis to the heart is very rare (*3–6*). In fact, metastatic heart tumors frequently originate from carcinomas of the bronchus and breast, malignant melanoma, lymphoma and leukemia (*7*). Heart involvement usually is detected by pericardial effusion with cardiac tamponade, tachy-

Received Aug. 29, 1997; revision accepted Mar. 18, 1998.

For correspondence or reprints contact: Yoshio Ishida, MD, Department of Radiology, National Cardiovascular Center, 5-7-1 Fujishirodai, Suita, Osaka 565-8565, Japan.

arrhythmias, atrioventricular block or congestive heart failure at the advanced stage (*7*).

We describe a patient with a history of uterine cervical carcinoma who presented with chest pain and electrocardiogram (ECG) abnormalities 3 yr after surgery. PET scanning with ^{18}F-fluorodeoxyglucose (FDG) revealed information about the nature and extent of metastases in the heart, lungs and lymph nodes of this patient.

CASE REPORT

A 36-yr-old woman who was diagnosed as having squamous cell carcinoma of the uterine cervix (clinical stage 1B) underwent radical hysterectomy and pelvic lymphadenectomy in April 1993. Surgery was followed by chemotherapy for 1 yr with oral UFT, a mixture of tegafur and uracil. The patient experienced no signs or symptoms for about 3 yr after surgery and then in January 1996 complained of right precordal pain at rest that increased on inspiration. A physical examination revealed no abnormal findings except lymph nodes swollen to 10 mm in the right lower neck. An ECG showed complete right-branch block with ST segment elevation in leads II, III, a V_f, V_1 to V_6 and negative T waves in leads V_3 to V_4. Since she had no previous history of organic heart disease and a normal ECG in November 1992, she was admitted to our hospital with suspected acute myocarditis and pericarditis.

After admission, levels of serum creatine phosphokinase, squamous cell carcinoma-related antigen and carcinoembryonic antigen were mildly elevated, but no infectious or inflammatory changes were detected. To examine the background of the ECG abnormalities, we performed echocardiography, which demonstrated an echogenic mass in the right ventricular myocardium with a small amount of pericardial effusion and a left ventricular ejection fraction of 60%. To evaluate the extent and property of the right ventricular tumor and other metastatic lesions, we performed electron beam CT (EBT), MRI, radionuclide imaging with ^{18}F-FDG, ^{67}Ga and ^{99m}Tc-sestamibi after we obtained the patient's informed consent and approval from the Institutional Review Board. At first, we scrutinized the right ventricular tumor. Contrast-enhanced EBT revealed an enlarged mass with soft-tissue density in the right ventricular myocardium (Fig. 1A). MRI also detected a mass with an intensity that was slightly lower than that of the myocardium and showed its invasion toward the pericardium (Fig. 1B). Fluorine-FDG PET imaging in the fasting state showed enhanced ^{18}F-FDG uptake in the right ventricular tumor, except for a small part of the tumor on the pericardial side and in the interventricular septum (Fig. 1C). We calculated the differential uptake ratio (DUR) on transaxial images, based on the equation described by Scott et al. (*8*):

(average ROI of the mass with the greatest concentration of ^{18}F-FDG in μCi/ml) $\times \sim$ (patient weight in kg)/(injected dose in mCi)

The DUR at the sites of high and negative ^{18}F-FDG uptake in the right ventricular tumor and of the remote normal myocardium were 7.19, 0.94 and 2.40, respectively. The extent of the left ventricular myocardial damage also was assessed by ^{99m}Tc-sestamibi SPECT imaging, which showed regional hypoperfusion in the left ventricular anteroseptal and septal walls but did not present regionally increased accumulation in the right ventricular tumor (Fig. 1D).

We next examined other metastatic lesions. Contrast-enhanced EBT showed a swollen lymph node in the para-aortic area and nodules measuring 9, 6 and 13 mm in diameter in right pulmonary segments S III, S V and S VI (*9*). In ^{18}F-FDG PET,

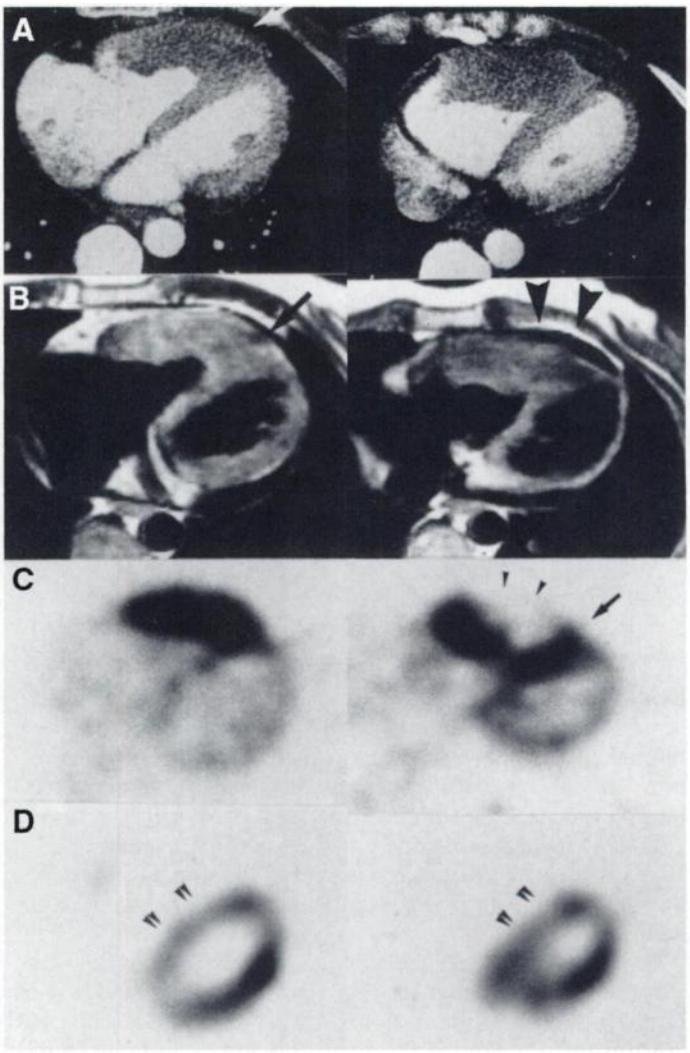

FIGURE 1. (A) EBT. Right ventricular tumor with soft-tissue density is slightly less enhanced by contrast medium than normal myocardium (white arrow). (B) MRI. It also demonstrates right ventricular tumor. Some pericardial effusion (large arrowheads) and loss of pericardial fat (large black arrow) suggest tumor invasion of pericardium. (C) Fluorine-18-FDG PET myocardial scan in fasting state shows high levels of ^{18}F-FDG accumulation in corresponding site to right ventricular tumor and also in interventricular septum (small black arrow). Fluorine-18-FDG uptake was decreased in part of right ventricular tumor (small arrowheads). (D) Technetium-99m-sestamibi myocardial SPECT. Mild perfusion defects are demonstrated in anteroseptal and septal myocardial regions (double arrowheads).

^{18}F-FDG uptake was enhanced in the lymph nodes at the para-aorta and the right lower neck and in S III and S VI of the right lung (Fig. 2A). Planar ^{67}Ga imaging did not reveal accumulation in the lymph nodes or pulmonary nodules, but it showed abnormal uptake in the right ventricular tumor (Fig. 2B). Also, planar ^{99m}Tc-sestamibi imaging did not show accumulation in the lymph nodes or pulmonary nodules (Fig. 2C).

Finally, a percutaneous myocardial biopsy revealed that the right ventricular tumor was squamous cell carcinoma of the same type as the original resected uterine cervical carcinoma. These findings suggested that the uterine cervical carcinoma had metastasized to the right ventricle, the interventricular septum and the lungs, as well as the cervical and para-aortic lymph nodes in this patient. Since further surgery was not indicated, she received three courses of chemotherapy with cisplatin, mitomycin C and vincristine. This strategy reduced the size of the right ventricular tumor and the volume of pericardial effusion. The ECG findings became normalized, and serum levels of squamous cell carcinoma-related antigen and

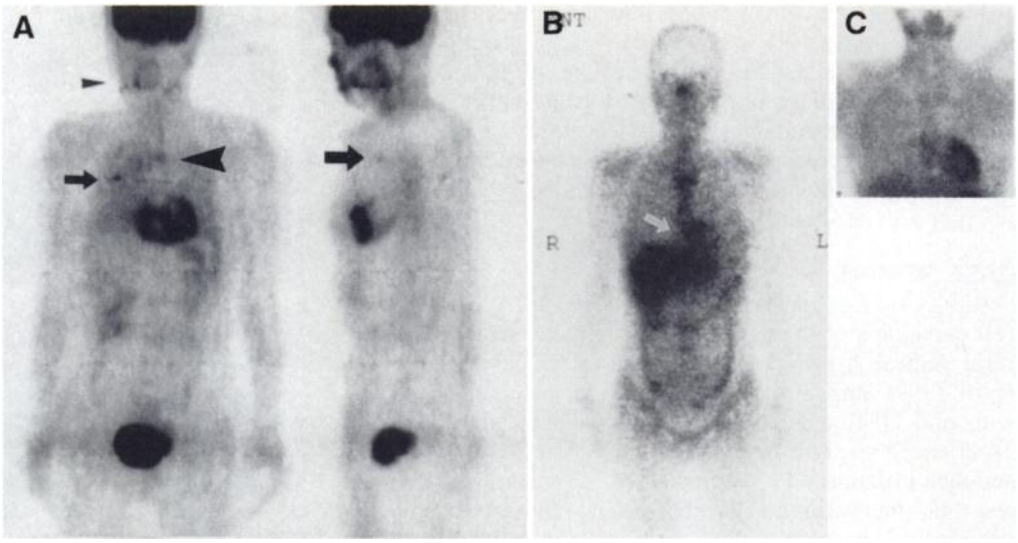

FIGURE 2. (A) Fluorine-18-FDG whole-body PET scan in the fasting state. Fluorine-^{18}F-FDG highly accumulated in heart, in S3 (large black arrow) and S6 (small black arrow) regions of right lung, lymph nodes at para-aorta (large arrowhead) and right lower neck (small arrowhead). (B) Planar ^{67}Ga scintigraphy. Abnormal uptake is shown in right ventricle (white arrow) but not in lungs and lymph nodes. (C) Technetium-99m-sestamibi anterior planar image. No accumulation is evident in right ventricle, lungs and lymph nodes.

carcinoembryonic antigen also reached the normal range. The patient has not yet been strong enough to tolerate another ^{18}F-FDG PET procedure.

DISCUSSION

Uterine cervical carcinoma rarely metastasizes to the heart through lymphatic or hematogenous channels (*3–6,10*). Autopsy studies have shown that the incidence of cardiac metastasis among patients with invasive uterine cervical carcinoma is 1.2% (11 incidents of metastasis among 922 patients) (*2,11*). While intracardiac metastasis is rarely symptomatic, this patient had abnormal ECG findings and complained of right precordal pain.

Fluorine-18-FDG PET clearly showed that the right ventricular tumor was malignant, and that it had extended to the interventricular septum. Echocardiography, EBT and MRI could barely discern the characteristics and extent of the tumor, although it was detected at high spatial resolution.

DUR is a useful marker with which to quantitatively distinguish malignant from benign or inflammatory lesions on ^{18}F-FDG PET images (*9,12,13*). The reported mean DUR is significantly higher for malignant, as opposed to benign lesions in pulmonary nodules (6.4 ± 0.56 versus 1.14 ± 0.26) (*9*). Patz et al. (*12*) used a DUR threshold of 2.5 to differentiate malignant from benign tumors in the lungs. In this study, the DUR of the region with high ^{18}F-FDG uptake in the right ventricular tumor was 7.19, indicating malignancy. On the other hand, ^{18}F-FDG PET showed that the tumor included regions with poor ^{18}F-FDG uptake with a DUR of 0.94. These regions indicate tumor necrosis, because high ^{18}F-FDG uptake generally represents viable malignant tumors versus necrotic tissue or fibrosis (*14*).

In addition to ^{18}F-FDG, ^{67}Ga is a useful tracer with which to detect malignancy. The reported sensitivity and specificity of ^{18}F-FDG PET and ^{67}Ga scintigraphy for detecting squamous cell carcinoma in the lungs or in the head and neck are 90%–100% and 88%–96%, respectively, and 76%–91% and 71%–96%, respectively (*12,13,15–18*). Lymph node metastases of squamous cell carcinoma with a diameter of less than 10 mm can be detected by ^{18}F-FDG PET (*13*). Although ^{67}Ga planar and SPECT images are equally sensitive in detecting pulmonary squamous cell carcinoma (70%–100% and 80%–100%, respectively), both procedures have problems in finding small lesions (*19,20*). The smallest lymph node metastasis shown by ^{67}Ga planar and SPECT imaging is 20 mm in diameter (*20,21*). In this study, both ^{18}F-FDG PET and ^{67}Ga scintigraphy detected a right ventricular tumor. Small metastatic lesions with a diameter more than 9, but not less than 6 mm, were distinguished by ^{18}F-FDG PET, whereas ^{67}Ga scintigraphy detected only those larger than 20 mm. Small metastatic lesions can be found more reliably by ^{18}F-FDG PET than by ^{67}Ga scintigraphy.

In this study, ^{99m}Tc-sestamibi failed to detect the right ventricular tumor and other metastatic lesions. This radionuclide has been used to diagnose cancer in the lungs, thyroid, brain, breast and bone, and the reported sensitivity for detecting lung squamous cell carcinoma is 85% (*22,23*). Since the exact mechanism of ^{99m}Tc-sestamibi accumulation in tumor cells is not well understood (*24*), the negative ^{99m}Tc-sestamibi uptake in the right ventricular tumor is difficult to explain. In this patient, ^{99m}Tc-sestamibi detected myocardial tissue damage of the interventricular septum that was probably due to tumor invasion.

CONCLUSION

We presented a rare example of a uterine cervical carcinoma that metastasized to the heart, lymph nodes and the lungs. Fluorine-18-FDG PET played an important role in defining a malignant tumor, evaluating its extent and viability and detecting small metastatic lesions.

REFERENCES

1. Willson JR. Malignant cervical lesions. In: Willson JR, et al., eds. *Obstetrics and gynecology*, 7th ed. St. Louis: CV Mosby Co.; 1983:622–629.
2. Peeples WJ, Inalsingh CHA, Hazra TA, Graft D. The occurrence of metastasis outside the abdomen and retroperitoneal space in invasive carcinoma of the cervix. *Gynecol Oncol* 1976;4:307–310.
3. Lustig V, Vlasveld LT, Bakker RH, Schreuder JE, Mooi WJ, Huinink WWB. Intracardiac metastasis, report of three cases. *Neth J Med* 1991;38:29–32.
4. Yanuck MD, Kaufman RH, Woods KV, Adler-Storthz K. Cervical carcinoma metastatic to the skull, heart, and lungs: analysis for human papillomavirus DNA. *Gynecol Oncol* 1991;42:94–97.
5. Cutrone JA, Georgiou D, Yospur LS, et al. Metastatic spread of cervical carcinoma to the right ventricle and pulmonary arteries: diagnosis by ultrafast computed tomography. *Am J Card Imaging* 1995;9:275–279.
6. Kountz DS. Isolated cardiac metastasis from cervical carcinoma: presentation as acute anteroseptal myocardial infarction. *South Med J* 1993;86:228–230.
7. Rosenthal DS, Braunwald E. Cardiac manifestations of neoplastic disease. In: Braunwald E, ed. *Heart disease*, 4th ed. Philadelphia: WB Saunders Co.; 1992:1752–1754.
8. Scott WJ, Schwabe JL, Gupta NC, et al. Positron emission tomography of lung tumors and mediastinal lymph nodes using fluorine-18-fluorodeoxyglucose. *Ann Thorac Surg* 1994;58:698–703.
9. Wegener OH. The lungs. In: Wegener OH, ed. *Whole body computed tomography*, 2nd ed. Boston: Blackwell Scientific Publications; 1993:182–187.
10. McAllister HA Jr. Tumors of the heart and pericardium. In: Silver MD, ed. *Cardiovascular pathology*, 2nd ed. New York: Churchill Livingstone; 1991:1297–1298.
11. Badib AO, Kurohara SS, Webster JH, Pickren JW. Metastasis to organs in carcinoma of the uterine cervix–influence of treatment on incidence and distribution. *Cancer* 1968;21:434–439.

12. Patz EF, Lowe VJ, Hoffman JM, et al. Focal pulmonary abnormalities: evaluation with fluorine-18-fluorodeoxyglucose PET scanning. *Radiology* 1993;188:487–490.
13. Braams JW, Pruim J, Freling NJM, Nikkels PGJ, Roodenburg JLN, Boering G, et al. Detection of lymph node metastases of squamous-cell cancer of the head and neck with FDG PET and MRI. *J Nucl Med* 1995;36:211–216.
14. Lamki LM. Tissue characterization in nuclear oncology: its time has come. *J Nucl Med* 1995;36:207–210.
15. Langhammer H, Glaubitt G, Grebe SF, et al. Gallium-67 for tumor scanning. *J Nucl Med* 1971;13:25–30.
16. Laubenbacher C, Saumweber D, Wagner-Manslau C, et al. Comparison of fluorine-18-fluorodeoxyglucose PET, MRI and endoscopy for staging head and neck squamous cell carcinomas. *J Nucl Med* 1995;36:1747–1757.
17. Muramatsu K, Yui N, Sawada K, Seki Y, Ishida I, Yui N. Clinical evaluation of gallium-67 scintigraphy for carcinoma of the lung: with special reference to prognosis. *Rinsho-Houshasen* 1986;3:41–47.
18. McKenna RJ, Haynie TP, Libshitz HI, Mountain CF, McMurtrey MJ. Critical evaluation of the gallium-67 scan for surgical patients with lung cancer. *Chest* 1985;87:428–431.
19. Broughton DL, Gibson CJ, Crake T, Pearce SJ, Leonard RCF. Gallium scanning by conventional imaging and emission computed tomography in the pretreatment evaluation of lung cancer. *Thorax* 1985;40:96–100.
20. Matsuno S, Tanabe M, Kawasaki Y, et al. Effectiveness of planar image and single photon emission tomography of thallium-201 compared with gallium-67 in patients with primary lung cancer. *Eur J Nucl Med* 1992;19:86–95.
21. DeMeester TR, Bekerman C, Joseph JG, et al. Gallium-67 scanning for carcinoma of the lung. *J Thorac Cardiovasc Surg* 1976;72:699–708.
22. Chiti A, Maffioli LS, Infante M, et al. Assessment of mediastinal involvement in lung cancer with technetium-99m-sestamibi SPECT. *J Nucl Med* 1996;37:938–942.
23. Aktolun C, Bayhan H, Pabuccu Y, Bilgic H, Husein, Koylu R. Assessment of tumour necrosis and detection of mediastinal lymph node metastasis in bronchial carcinoma with technetium-99m sestamibi imaging: comparison with CT scan. *Eur J Nucl Med* 1994;21:973–979.
24. Mariani G. Unexpected keys in cell biochemistry imaging: some lessons from technetium-99m-sestamibi. *J Nucl Med* 1996;37:536–538.

PET Evaluation of Therapeutic Limb Perfusion in Merkel's Cell Carcinoma

Jose L. Lampreave, François Bénard, Abass Alavi, Jose Jimenez-Hoyuela and Douglas Fraker
Division of Nuclear Medicine and Department of Surgery, University of Pennsylvania Medical Center, Philadelphia, Pennsylvania

An 87-yr-old woman diagnosed with recurrent Merkel's cell carcinoma was treated with therapeutic limb perfusion and underwent PET scanning with ^{18}F-fluorodeoxyglucose (FDG). PET studies were obtained before and after treatment to determine the response to the intervention. A baseline whole-body study was obtained to assess the extent and degree of disease activity. This was followed by a repeat PET scan 2 mo later after treatment with isolated limb chemotherapy with high-dose melphalan and tumor necrosis factor-α. The initial scan demonstrated multiple foci of high FDG uptake in the left calf, a left supraclavicular lesion and also detected concurrent keratinizing squamous cell metastasis in the right axilla. A repeat PET study showed complete metabolic resolution of the lesions in the left calf after treatment. FDG PET may be a useful technique for staging Merkel cell carcinoma and for assessing the tumor response after therapy of this rare tumor.

Key Words: Merkel cell carcinoma; PET; fluorine-18-fluorodeoxyglucose; isolated limb perfusion

J Nucl Med 1998; 39:2087–2090

Merkel cell carcinoma is a rare neuroendocrine tumor derived from cells located in the basal layers of the epidermis. This tumor is thought to be either of neural or epidermal origin (*1*). It typically presents as violaceous nodules in sun-exposed skin of elderly people (*2*). The local recurrence rate has been estimated at 26%–44%, and nearly three-fourths of the patients develop local nodal involvement (*3*). Another one-third present distant metastases to the liver, bone, brain, lung or skin (*4*). While most published data are supportive of wide surgical excision of the tumor with radiotherapy, the treatment remains controversial, and it is not clear whether removal of clinically silent regional lymph nodes is justified (*3*). We report a case of Merkel cell tumor studied with ^{18}F-fluorodeoxyglucose (FDG) PET before and after isolated limb perfusion (*4*).

Received Apr. 23, 1997; revision accepted Aug. 14, 1998.
For correspondence or reprints contact: Abass Alavi, MD, Division of Nuclear Medicine, Hospital of the University of Pennsylvania, 3400 Spruce St., Philadelphia PA 19104.

CASE REPORT

An 87-yr-old woman with a history of Merkel's cell tumor in her left lower extremity underwent FDG PET scanning because of possible recurrent and metastatic disease. The tumor had been removed in 1995 with a wide excision and superficial and deep inguinal lymph node dissection and then treated with adjuvant radiation therapy. After this treatment, she had considerable leg edema. She developed increased swelling in the calf and ankle with extensive, subtle, erythematous, plaque-like lesions that became extremely painful. Needle biopsy of these areas demonstrated recurrent Merkel's cell tumor. Her past medical history was significant for asthma, coronary artery disease, atrial fibrillation, deep venous thrombosis and hypertension. At the time of admission she was on diltiazem hydrochloride, hydrochlorothiazide and theophylline. Physical examination demonstrated an edematous left lower extremity with a diffuse area of erythematous plaques over the prior excision site. There were no other areas of disease noted with the exception of multiple basal skin cancers on the face, shoulder and back.

An FDG PET scan was requested to determine the extent of the disease within the limb as well as systemically.

MATERIALS AND METHODS

A PENN-PET scanner (*5*) with a resolution of 5.5 mm in all three planes was used to perform a whole-body scan. Two hours after the intravenous injection of 114 mCi/kg FDG, a whole-body PET study was obtained over the chest, abdomen and entire lower limbs. At the time of this study, rapid transmission scans using a single, photon-emitting ^{137}Cs source were not yet available (*6*). Therefore, no transmission scan was obtained in this study to minimize patient discomfort considering the lengthy (neck-to-toe) emission acquisition. The final images were reconstructed with the ordered subsets expectation maximization algorithm, according to a previously reported technique (*7*). On visual interpretation, areas of focally increased activity that did not correspond to the normal distribution of FDG (such as kidneys, ureters, muscles, etc.) were rated as abnormal. No quantitative measurements were used to